Optics Communications 284 (2011) 2131–2136

Contents lists available at ScienceDirect

Optics Communications

journal homepage: www.elsevier.com/locate/optcom

Frequency signature of water activity by biospeckle laser

Rafael Rodrigues Cardoso, Anderson Gomide Costa, Cassia Marques Batista Nobre, Roberto Alves Braga Jr. *

Universidade Federal de Lavras (Brazil) CP 3037 Lavras MG 37.200-000, Brazil

ARTICLE INFO

Article history:
Received 22 September 2010
Received in revised form 2 January 2011
Accepted 4 January 2011
Available online 14 January 2011

Keywords:
Dynamic speckle
Spectral
Isolation

ABSTRACT

Biospeckle laser technique has become an important tool to investigate biological activity in several areas of science. However, due to the complexity of biological materials it is necessary to develop research processes that ensure greater efficiency in isolating areas of different activities in the same material using the biospeckle. Thus, alternative techniques, such as those related to spectral domain, allow approaches that provide a means for frequency and isolation marking of various observed phenomena. The possibility of creating frequency markers related to physical or chemical phenomena under biospeckle laser monitoring opens the way for important applications in the analysis of biological materials. In seeds, for example, one research challenge is the creation of a methodology to analyze their vigor undermining the influence of water activity. This study aimed to use wavelet transform to create maps in frequency of biological material, particularly from maize and bean seeds, seeking to isolate water activity. Wavelet transform was used in conjunction with traditional biospeckle laser methods, Fujii, Generalized Differences and Time History Speckle Patterns. The data analysis allowed access of information in different frequencies, making it possible to map activities that only occur at certain frequencies in the seeds associated to particular areas they operate, as in the case of activities present in the embryo as well as those present in the endosperm. Thus the work enabled the identification of frequency bands where water activity may be operating creating a signature useful in further works.

1. Introduction

Methods of analysis which use non-destructive techniques have been of great importance in the evaluation and monitoring of biological properties. That's why biospeckle laser (BSL) has become over the years an increasingly efficient application for monitoring activity, particularly in the areas of biology, medicine and agriculture [1]. In agriculture, we find works that use BSL in fruit analysis [2], in seed and fungi analysis [3,4], in leaves of coffee moisture monitoring [5], in root growing observation [6] and in works with animal semen evaluation [7]. The biospeckle technique, also known as dynamic laser speckle, is based on monitoring changes in interference patterns prominent from illumination over time by a coherent light, in particular the laser [8]. The changes mentioned before are related to the movement of dispersors of light which can be either within the cells or external of them. In most cases, the water content, or water activity, will be one of the main contributors of the level of activity [9]. The routine methods proposed to analyze the activity through BSL technique are based on the summation of all contributions related to a wide range of phenomena, thus without the ability to separate or isolate a particular feature [10]. There are many approaches to achieve the final result of the multiple interferences expressed by the BSL, and they can be divided in on-line and off-line techniques. The on-line techniques are based on the single-exposure speckle photography [11,12], also known as Laser Speckle Contrast Imaging field (LSCI). The alternatives to the absence of the time history are presented by the Time Laser Speckle Contrast Imaging field (TLSCI), also known as Laser Speckle Temporal Contrast Analysis (LSTCA) [13], or in the field of the off-line techniques which are mainly discussed in this work. The great limitation of not being able to access the final activity without the identification of the main contributors demanded alternative ways to split the original signal into subsignals which can be linked to any particular feature or even to enhance the results by avoiding or damping some undesirable information. One case of splitting separated the levels of grey scales in the images by means of three thresholding ranges through fuzzy approaches [14]. Another way to go further into the separation of signals adopted spectral ranges as a feasible alternative [15], which was improved by the use of the wavelets transform [16,17], and with the implementation of Entropy as an alternative to Inertia Moment [17]. The adoption of the Cross-Spectrum theory was an additional tool in the spectral domain [18], which was compared to the Inertia Moment and Entropy [19] regarding the frequency point of view. It was presented that Entropy and Cross-Spectrum offered better answers for low frequency components in the original signal while Inertia Moment was better with high frequency components. The huge absence of time information in the LSCI or even the low amount of images in the LSTCA is the main limitation to these techniques to the adoption of the

* Corresponding author. Tel.: +55 35 3829 1672.
E-mail addresses: robbraga@deg.ufla.br, robbraga@gmail.com (R.A. Braga).

0030-4018 © 2011 Elsevier B.V. Open access under the Elsevier OA license.
doi:10.1016/j.optcom.2011.01.003

spectral approaches. The challenge of isolation [10] was in turn a great motivation in this field with many relevant applications, in particular in the seed analysis area where it is possible to see many efforts to deal with it using digital imaging information technology [20]. This work aimed to present steps to achieve actual isolation of biological phenomena by means of spectral approaches associating them to graphical and numerical routine methods.

2. Theory

2.1. Graphical analysis of the biospeckle

Among the routine methods to analyze graphically the biospeckle one can highlight the Fujii approach [21] and the Generalized Differences Method [22]. Fujii's method is based on the visibility calculation among the pixels of images recorded over time. The procedure for the construction of the Fujii method is described by Eq. (1).

$$I(x,y) = \sum_k \left| \frac{I_k(x,y) - I_{k+1}(x,y)}{I_k(x,y) + I_{k+1}(x,y)} \right| \quad (1)$$

where $I_k(x,y)$ is the intensity value at image k and position (x,y). From Eq. (1) a new image is constructed, and the pixels assume in the final map a value close to zero on the gray shades scale in areas where there were no changes in intensity over time, and higher values, near 255 in areas where the pixels went through big changes. The Generalized Difference Method (GD) is a derivative technique from the Fujii method without the denominator and with a recursion on the differences. In the GD, what is done is to perform a sum of intensity differences between an image and its subsequent. The resulting image can be expressed by Eq. (2).

$$I(x,y) = \sum_k \sum_l |I_k(x,y) - I_{k+l}(x,y)| \quad (2)$$

where k and l are the numbers of the images in the image series. The double summation demonstrates one difference in the Fujii method which in this case each image is compared with all the others, requiring more computational effort.

2.2. Numerical analysis of biospeckle

An approach to numerically analyze the images of a tissue from laser illumination consists in the creation of the Time History Speckle Pattern or THSP. The construction of THSP was proposed from a pseudotemporal image concept [23] and from a space–time speckle [24]. The standard THSP is formed when only one row or column is repeatedly captured in the speckle images at a certain sampling rate and then these strips are placed side by side forming a new image. With THSP it is possible to estimate the degree of activity of an illuminated object based on dynamic speckle behavior. Most of the techniques described in existing literature are based on obtaining a single numeric value from THSP. This value can be obtained by applying auto-correlation, or through the Inertia Moment (IM) [25], which results in a second-order statistic. Inertia Moment (IM) values are obtained from the creation of a co-occurrence matrix that is defined by Eq. (3)

$$COM = \left[N_{ij}\right]. \quad (3)$$

Where N_{ij} is the number of occurrences of the gray level i followed by the gray level j over the time dimension in the matrix THSP, where COM is a matrix of 256×256. The Inertia Moment values are defined by Eq. (4).

$$IM = \sum_i \sum_j \left(\frac{N_{ij}}{\sum_j N_{ij}} \right) * (i-j)^2. \quad (4)$$

2.3. Spectral entropy

Spectral entropy can be obtained from the Fourier power spectrum, which is a way to verify the order of a signal, i.e. A system that possesses periodicity exhibits a peak in the frequency-domain. Therefore the frequency range (band) concentration in a single peak corresponds to low values of entropy. On the other hand, non-regular activities provide spectral components over a wide range of the frequency-domain, resulting in high entropy [17]. Transformation of the signal to the frequency-domain can be performed directly by the Fourier transform, or specifically by the wavelet transform that allows more information about the frequencies in time. By using Discrete Wavelets Transform to study the biospeckle, the lines of THSP are divided in temporal windows and the wavelets average energy can be obtained from Eq. (5) [17].

$$E_j^{(i)} = \frac{1}{N_j} \sum_{k=0}^{(L/2^j)-1} |C_{k,j,i}|^2. \quad (5)$$

Where:

- $i = 1, ..., NT$, and NT = signal length/L, which is the size of the temporal window.
- N_j: number of Wavelet coefficients at j level of resolution, including i time interval.

The total energy in the i time interval can be obtained by Eq. (6), being that the Wavelets energy pertaining the ith window at the THSP line can be obtained by Eq. (7), and the Shannon entropy at the ith window by Eq. (8). [17].

$$E_{total}^{(i)} = \sum_{j<0} E_j^{(i)} \quad (6)$$

$$p_j^{(i)} = \frac{E_j^{(i)}}{E_{total}^{(i)}} \quad (7)$$

$$S_{WT}^{(i)} = -\sum_{j<0} p_j^{(i)} ln|p_j^{(i)}|. \quad (8)$$

3. Material and methods

3.1. Backscattering configuration

The experimental configuration adopted was the backscattering as presented in Fig. 1, where the computer was responsible for assembling the images from the CCD camera with a time rate of acquisition set up in

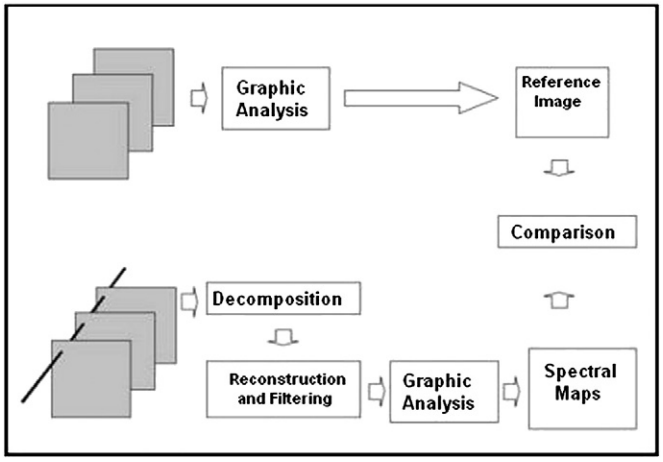

Fig. 1. Experimental setup for seed lighting.

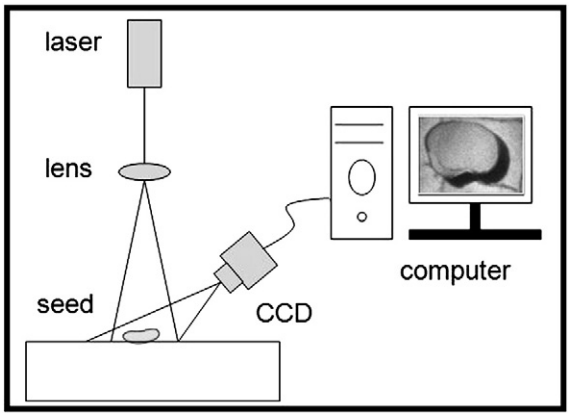

Fig. 2. Flowchart representing the analysis with filtering process.

0.08 s. The maximum frequency that could be observed, based on the sampling theory, was $1/(2\times0.08)$ s which was related to 6.25 Hz. The number of frames assembled varied in the experiments but all of them were expressed in base of 2, in particular 64 and 128 frames, in order to implement the fast fourier transform algorithm.

3.2. Illuminated samples

The biological materials chosen to be illuminated were bean and corn seeds. The corn seeds had moisture over 20% of wet base and the bean seeds with different levels of moisture, as well as in two biological stages, one collection alive and another dead. The bean seeds were tested in accordance with their viability and a dead parcel was separated from a living parcel. Both the dead and living seeds were put in wet paper for 12 h and then they were let loose in water at room temperature.

3.3. Graphical analysis

The graphical analysis was conducted in two ways. One was when routine methods, such as GD and Fujii, were implemented without any processing of the original images and the second way was when routine methods were implemented in the collection of primary images after the filtering process. The two filtering processes implemented damping of one range per time and reconstructing the image, and damping all the ranges except one which was used as the base for the reconstruction of the resulting image. In Fig. 2 it is possible to see the two paths followed in the graphical analysis. The graphical analysis was implemented in the corn and bean seeds. The protocol of filtering used the wavelets transform [6] and the number of frequency ranges varied in accordance to the number of images assembled. The inverse wavelet transform was performed in two ways to reconstruct the images: reconstructing the images on just one frequency band, and reconstructing the images by eliminating only one frequency band. For the maize seed, 64 images of 256×490 pixels were used and it was possible to obtain results in 21 frequency bands between 0 and 6.25 Hz. For the bean seeds, 128 images of 486×469

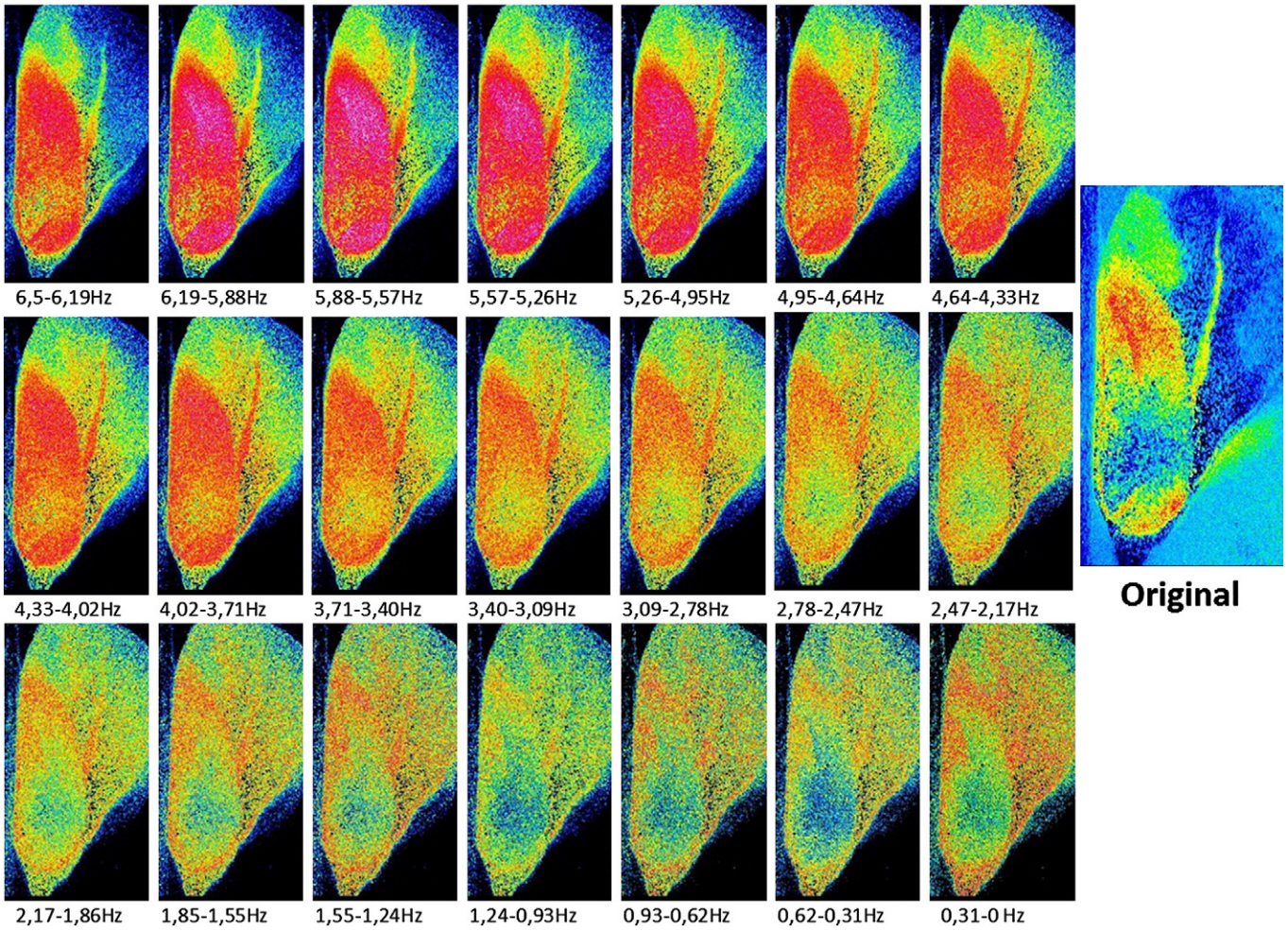

Fig. 3. Results of Fujii in maize seeds with filtering reconstructing just one frequency range, with the larger image on the right representing the image control without any filtering.

pixels were used. In turn, the reconstruction of the images to generate spectral maps was performed in order to reconstruct the images on just one frequency band at a time. From the 128 original images, it was possible to obtain 25 frequency bands between 0 and 6.25 Hz.

3.4. Numerical analysis

THSP live bean seeds were analyzed in two different stages, one which we will call the initial stage where the seed is saturated with water and the other referred to as the final stage where the seed reached hygroscopic equilibrium with the environment. We sought to evaluate the behavior of water activity from the initial stage to final stage. Inertia Moment and Entropy techniques associated with wavelet transform were applied for filtering and reconstruction of the data. The frequency bands were rejected one by one and then compared to the original not rejecting any frequency range.

4. Results and discussions

4.1. Graphical analysis

Fig. 3 shows the result of processing the method of Fujii in maize seed with filtering and reconstruction of only one frequency band. The image control on the right in Fig. 3 represents the result of the process without any filtering, where on the bottom left of the seed, the embryo is found with activities represented by the colors red and yellow, and on the top right of the seed, the endosperm is found with low activity represented mainly by blue and green colors. The 21 frequency bands, presented in the first images, show the embryo evidenced in red, which means high activity at high frequencies, while in the last images the endosperm is highlighted in red at low frequencies as was also shown in an earlier work [15]. The use of only one band for the Fujii processing shows that the phenomena that constitute the biospeckle are selective, in other words, they are restricted to narrow bands of frequency improving phenomena isolation, opening up a potential application in many biological materials that demand isolation areas of activity. The observed activity in the endosperm can be attributed to the presence of water in tissue without biological activity. This isolation of water activity in the observed data in the biospeckle is of great relevance to the improvement of the results of seed analysis once the activity promoted by the water in tissue masks the observation of metabolic activities of tissues that makes it difficult to compare and identify living and dead tissues. The separation of the results of Fujii in various frequency ranges allow for isolated forms of observation of the phenomena that are not possible in the original image. An example of this ability is observed in the embryo where at low frequencies a well-defined area of low activity is observed in the center of the embryo, which does not occur at high frequencies showing that in the original image the result undermined this information. In turn, the obtained results by eliminating only one frequency band showed no difference from the original image not presented here graphically. This is due to the fact that only one frequency band is not able to alter the final results due to its low energy which is not perceived by processing Fujii, especially in visual form. In the presented results in Fig. 3, it is still possible to observe that there is a range of activity in the endosperm in the central part of the image represented by an active band, in yellow, in the original image processed. This band is related to a crack in the endosperm, and thus a greater activity in this area, where there should normally be less activity, which can be attributed to greater water evaporation. From the images in frequency it is possible to conclude that evaporation in greater activity areas generates high frequency answer in the speckle patterns, showing the signature in frequency of the evaporation phenomenon. The mapping of a bean seed where there is no such clear separation from the embryo and endosperm, as occurs in the corn seed, is shown in Fig. 4 reconstructing only one frequency band. The result shows an area in the seed that operates at a higher rate in the high frequency

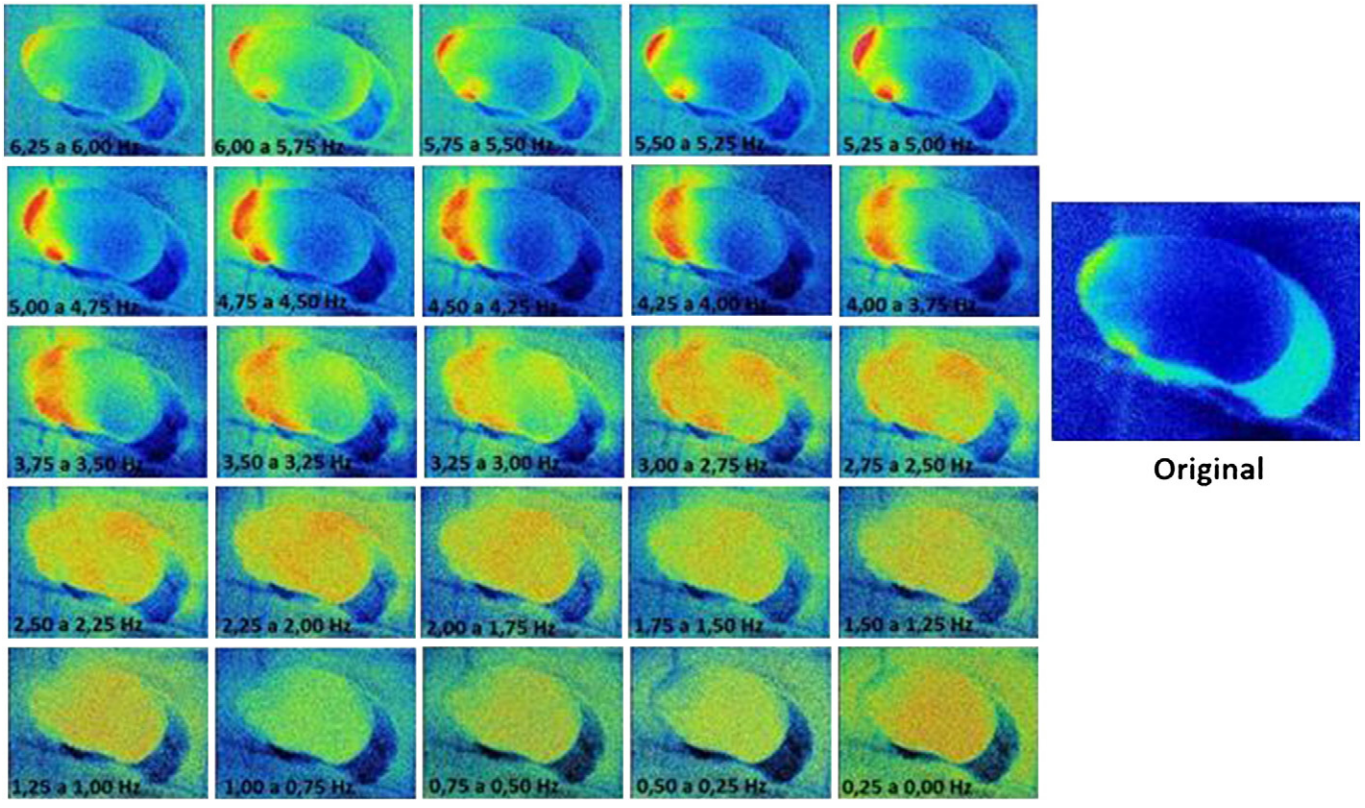

Fig. 4. Partial result obtained with the bean seed with mechanical damage, with image control on the right.

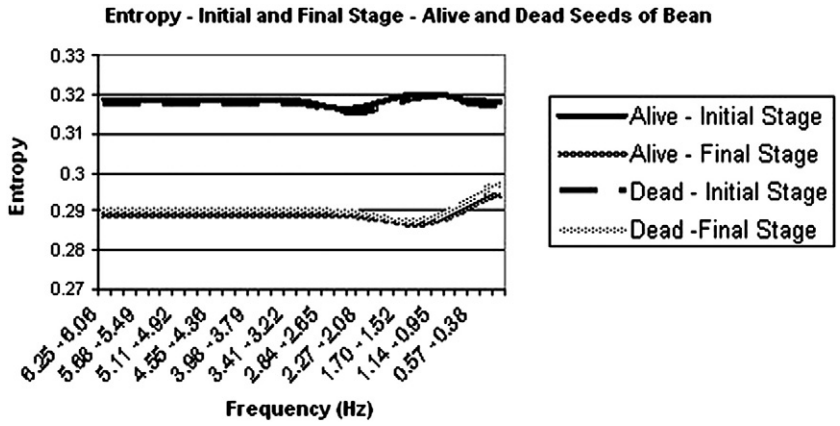

Fig. 5. Behavior of entropy in living and dead bean seeds with high and low water activity.

bands that are related to a portion of the seed attached to higher biological activity during germination. The control image, without any filtering, is in the right of Fig. 4. It was also noted that there is some phenomena occurring in all seeds from the medium to the lowest frequencies, which is related to the water activity characterized as a signature in frequency which is also seen in the corn. To confirm this hypothesis, and seeking separation of water activity in relation to the cellular activity, the numerical analysis occurred with the THSP's bean seed combining the IM techniques and entropy with spectral analysis.

4.2. Numerical analysis

The numerical analysis that showed best results were those in which the reconstructions were based on the elimination of only one frequency band opposing the achieved ones in the graphical analysis. Our ability to analyze numerical values more efficiently than images, and the different routine techniques of graphic and numeric processing, may explain the difference in the reconstruction approach.

4.2.1. Entropy

In Fig. 5 we analyze the behavior in living and dead bean seeds in their initial stage, in other words, with high water activity and then finally with low water activity. As already evidenced, [19] entropy is only able to monitor changes in speckle patterns related to low frequencies, which in Fig. 5 represent the bands below 3.41 Hz. Entropy behavior, in both living and dead seeds in stages of high water activity and low water activity, is the same at low frequencies, which shows that in these frequency bands only the water is capable of expressing changes in speckle patterns. In Fig. 5 it is possible to notice a clear separation of entropy in the initial stage of higher water activity in relation to the final stage where the present water in the seed is already in small quantities. In this case, lower entropy observed in the stages of lower water activity is related to phenomena with greater stability, in other words, less random activity, which is directly related to the mobility that water gives to the member components of plant tissue, and nor to the evaporation. The entropy change, in the bands of 3.41 Hz to 0.0 Hz, can be linked to the type of chemical bond that the water has, but their classification still remains a challenge. Finally, in Fig. 5, it is possible to observe that the entropy differences of live and dead seeds are small, at low frequencies, which leads us to conclude that the biological activity is not relevant in the speckle patterns changes in this spectral band. These achievements are an advance to that presented in other account [10] using the same data. However, in this work the access to the signatures was only possible since the graphical analysis were combined to the numerical answers. In addition, in this work, the whole picture was formed by the adoption of the concepts of absorbed, solvent, adsorbed and constitution water in order to correlate them to the frequency behavior.

4.2.2. Inertia moment

In Fig. 6 you can notice that by removing the frequencies located in the high frequency band there is a reduction of activity in the seed, occurring sharply in the initial stage when the water concentration is greater inside of it, and occurring less sharply in the final stage when the water concentration is lower inside the seed. We relate this phenomenon to water loss during evaporation as the biological activity of the seed itself, as also noted in the corn seed, in particular in the region of the crack, as being more conducive to more intense evaporation. This phenomenon is linked to high frequencies, which explains the greater attenuation observed. In inverse form of entropy, [19] IM has the ability to monitor changes in high frequencies and a low capacity for monitoring phenomena at low frequencies. The

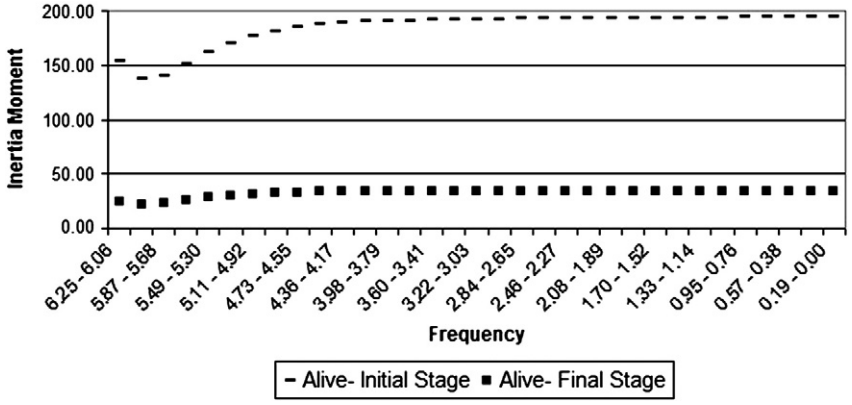

Fig. 6. Behavior of the Inertia Moment in dead seeds with high and low water activity.

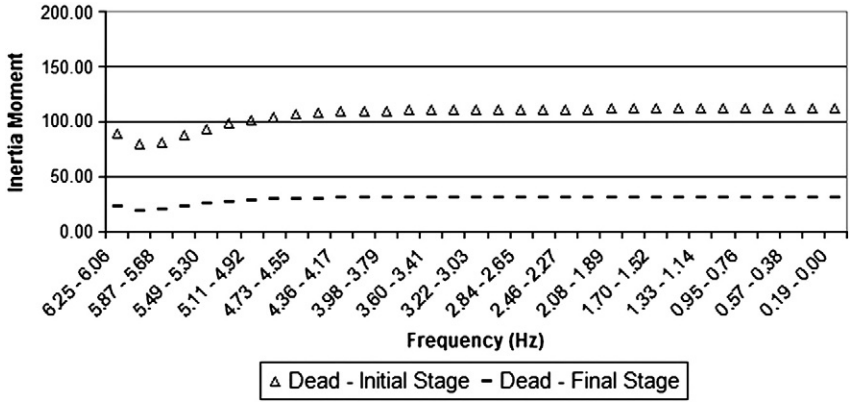

Fig. 7. Behavior of the Inertia Moment in dead seeds with high and low water activity.

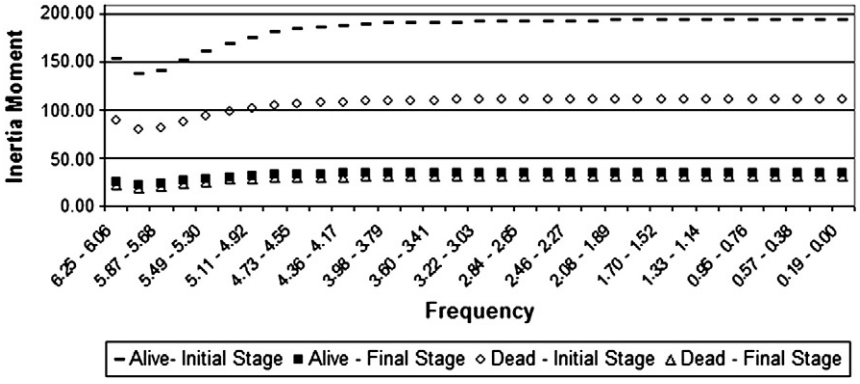

Fig. 8. Behavior of the Inertia Moment in live and dead bean seeds with high and low water activity.

achieved results in dead bean seeds with high and low water activity (Fig. 7) were similar to those found in living seeds reaffirming that even in high-frequencies the water has influence, and in this case, strongly linked to intense evaporation as observed in the graphical analysis. Fig. 8 also reinforces the hypothesis of the biological activity influence throughout the speckle frequency in the seeds. However, it is clear that to carry out separated analysis of biological activity in seeds from the water activity it is necessary to avoid the initial phase of intense evaporation even when carrying out the filtering. The influence of water, tear in that case, was also observed in a study to analyze the ocular microtremor by speckle approach [26]. In the corn seed, the most intense evaporation occurred at the crack can be linked to the intermediate bands helping future work, since it can be labeled as a signature of the evaporation of the water. Does the evaporation water cause biospeckle activity in that band of frequency in all the cases?

5. Conclusions

This work presented steps to achieve actual isolation of biological phenomena by means of spectral approaches associating them to graphical and numerical routine methods. The observation of water activity in different spectral ranges, and the evaluation of routine methods, presented novel information of the effort related to the separation of the phenomena responsible for the biospeckle patterns.

Acknowledgements

Special thanks to Federal University of Lavras, to FAPEMIG, to CNPq and to Finep.

References

[1] H. Rabal, R.A. Braga, Dynamic Laser Speckle and Applications, CRC Press, New York, 2008.
[2] G.F. Rabelo, R.A. Braga, Rev. Bras. Eng. Agric. Ambient 09 (2005) 570.
[3] R.A. Braga Jr., I.M. DalFabbro, F.M. Borem, G.F. Rabelo, R. Arizaga, H.J. Rabal, M. Trivi, Biosyst. Eng. 86 (2003) 287.
[4] R.A. Braga Jr., G.F. Rabelo, L.R. Granato, E.F. Santos, J.C. Machado, R. Arizaga, H.J. Rabal, M. Trivi, Biosyst. Eng. 86 (2005) 465.
[5] J.L. Botega, R.A. Braga, Rev. Bras. Eng. Agric. Ambient 13 (2009) 483.
[6] R.A. Braga, L. Dupuy, Eur. Biophys. J. 38 (2009) 679.
[7] P.H. Carvalho, J.B. Barreto, R.A. Braga Jr., G.F. Rabelo, Biosyst. Eng. 102 (2009) 31.
[8] M.R. Trivi, in: H.J. Rabal, R.A. Braga (Eds.), Dynamic Laser Speckle and Applications, CRC, 2008, p. 21.
[9] R.A. Braga, G.F. Rabelo, J.B. Barreto, F.M. Borem, J. Pereira, M. Muramatsu, I.M.D. Fabbro, in: H.J. Rabal, R.A. Braga (Eds.), Dynamic Laser Speckle and Applications, CRC, 2008, p. 181.
[10] R.A. Braga, G.W. Horgan, A.M. Enes, D. Miron, G.F. Rabelo, J.B. Barreto, Comput. Electron. Agric. 58 (2007) 123.
[11] J.D. Briers, Opt. Commun. 13 (1975) 324.
[12] A.F. Fercher, J.D. Briers, Opt. Commun. 37 (1981) 326.
[13] P. Li, S. Ni, L. Zhang, S. Zeng, Q. Luo, Opt. Lett. 31 (2006) 1824.
[14] A. DaiPra, I. Passoni, H.J. Rabal, Signal Process. 89 (2009) 266.
[15] I.L. Sendra, R. Arizaga, H. Rabal, M. Trivi, Opt. Lett. 30 (2005) 1641.
[16] M.F. Limia, A.M. Núñez, H. Rabal, M. Trivi, Appl. Opt. 32 (2002) 6745.
[17] I. Passoni, A. Dai Pra, H.J. Rabal, M. Trivi, R. Arizaga, Opt. Commun. 246 (2005) 219.
[18] R.A. Braga Jr., W.S. da Silva, T. Sáfadi, C.M.B. Nobre, Opt. Commun. 281 (2008) 2443.
[19] C.M.B. Nobre, R.A. Braga Jr., A.G. Costa, R.R. Cardoso, W.S. da Silva, T. Sáfadi, Opt. Commun. 282 (2009) 2236.
[20] A. DellAquila, Agron. Sustainable Dev. 29 (2009) 213.
[21] H. Fujii, T. Asakura, Opt. Lett. 10 (1985) 104.
[22] R. Arizaga, N. Cap, H.J. Rabal, M. Trivi, Opt. Eng. 41 (2002) 287.
[23] A. Oulamara, G. Tribillon, J. Duvernoy, J. Mod. Opt. 36 (1989) 165.
[24] Z. Xu, C. Joenathan, B.M. Khorana, Opt. Eng. 34 (1995) 1487.
[25] R. Arizaga, M. Trivi, H. Rabal, Opt. Laser Technol. 34 (1999) 1487.
[26] M. Alkalbani, E. Mihaylova, N. Collins, V. Toal, Proc. SPIE 7176 (2009) 717606.